Example 7.4 Elastoplastic analysis of a raft resting on Continuum medium

1 Description of the problem

One of the difficulties by applying the Continuum model to practical problems is the appearance of the high contact pressures at the raft edges, especially when the raft carries heavy loads. The appearance of plastic zones at the raft edges is related to the traditional mathematical soil models used in the analysis, which depend on the theory of elasticity. Therefore, an application example is carried out to show the applicability of the developed nonlinear analysis to redistribute the high contact pressures at the edges of both elastic and rigid rafts.

A rectangular raft with dimensions of 8 × 16 [m^2] is chosen and subdivided into 512 square elements. Each element has a side of 0.5 [m] as shown in Figure 7.13. The raft carries a uniform load of 600 [kN/m^2].

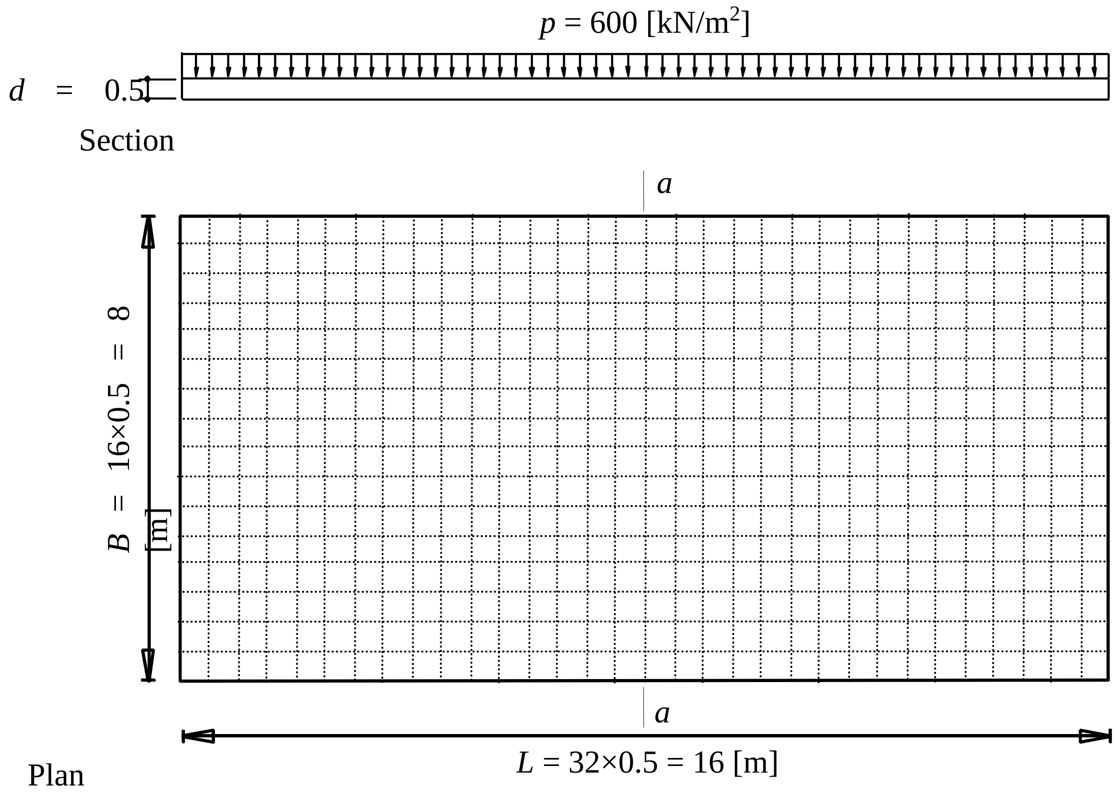

Figure 7.13 Raft geometry, loading and FE-Net

2 Soil properties

The raft rests on a homogeneous sand layer of thickness 10 [m], overlying a rigid base. The sand layer was supposed to have the following parameters:

Modulus of compressibility	E_s = 12 000	[kN/m^2]
Poisson's ratio	ν_s = 0.25	[-]
Unit weight	γ_s = 17.5	[kN/m^3]
Angel of internal friction	φ = 27.5	[°]
Cohesion	c = 0.0	[kN/m^2]
Foundation depth under the ground surface	t_f = 0.5	[m]

3 Raft material and thickness

The raft material and thickness were supposed to have the following parameters:

Raft thickness	d = 0.5	[m]
Young's modulus	$E_b = 3 \times 10^7$	[kN/m^2]
Poisson's ratio	ν_b = 0.15	[-]
Unit weight	γ_b = 0.0	[kN/m^3]

Unit weight of the raft is chosen γ_b = 0.0 [kN/m^3] to neglect the self-weight of the raft.

4 Analysis

The nonlinear analysis of the raft was carried out for both elastic and rigid rafts on Continuum medium. Two cases concerning the ultimate bearing capacity q_{ult} are considered as follows:

i) The ultimate bearing capacity q_{ult} is uniform.
Its value is obtained from Equation 7.6, q_{ult} = 1603 [kN/m^2]

ii) The ultimate bearing capacity q_{ult} is variable.
The ultimate bearing capacity q_{ult} at the raft edges is determined from the second term of Equation 7.6, $q_{ult} = \gamma_1\ t_f\ N_d\ \nu_d$ = 951 [kN/m^2], while the ultimate bearing capacity q_{ult} at the raft center is determined from Equation 7.6 when the third term is doubled, $q_{ult} = \gamma_1\ t_f\ N_d\ \nu_d + 2\ \gamma_2\ B\ N_b\ \nu_b$ = 1753 [kN/m^2]. Figure 7.14 shows the contour lines of the variable ultimate bearing capacity q_{ult}

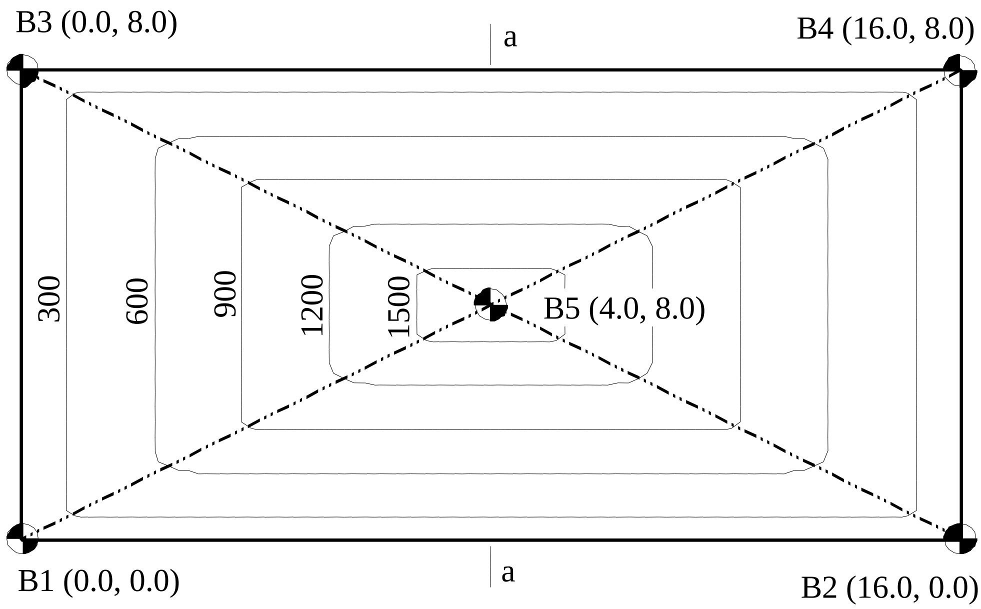

Figure 7.14 Contour lines of the variable ultimate bearing capacity q_{ult} [kN/m^2]

Unfortunately, until now there is no available method to determine the bearing capacity of the soil for irregular contact pressure, where the bearing capacity equations are derived for a uniform contact pressure under the foundation. In this example, the variability of q_{ult} under the raft is chosen according to the principle of equilibrium forces acting on the raft and the soil at the failure. In which, the part of ultimate bearing capacity from the second terms in Equation 7.6 is uniform. This part represents the influence of the applied pressure beside the foundation, $\gamma_1\ t_f\ N_d\ \nu_d$. The part of ultimate bearing capacity from the third term in Equation 7.6 has a triangle cross-section at the middle of the raft (Figure 7.15). This part represents the influence of the foundation geometry, $\gamma_2\ B\ N_b\ \nu_b$.

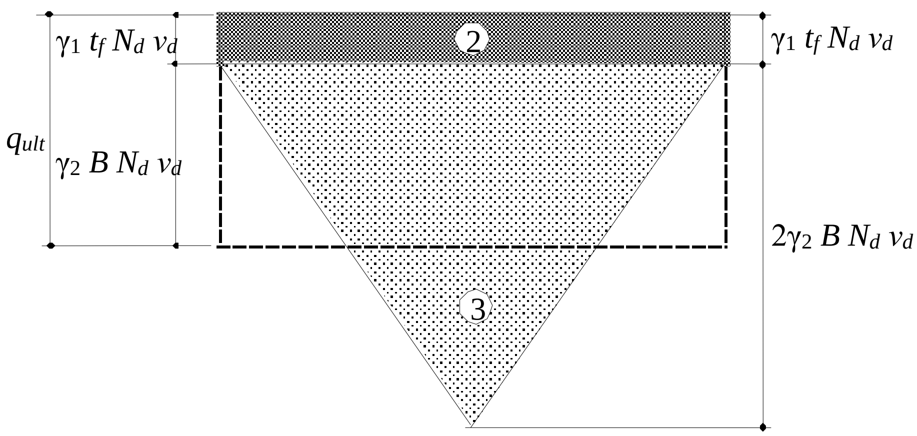

Figure 7.15 Ultimate bearing capacity at the soil failure (section a-a)

5 Results and discussions

The contact pressures q at section a-a of the raft in case of uniform q_{ult} are shown in Figures 7.16 and 7.17, while those in case of variable q_{ult} are shown in Figures 7.18 and 7.19. These figures show that the linear analysis of the both elastic and rigid rafts gives high contact pressures at the raft edges. As it is expected due to the nonlinear analysis, the contact pressures shift from the edges to the center of the raft, and this leads to a loss of the bearing capacity. Figures 7.16 and 7.17, which represent case of uniform q_{ult} show that although the contact pressures over all nodes on the raft are less than the ultimate bearing capacity limit, but the contact pressures at the raft edges still higher than those at the center. In contrast for case of variable q_{ult} the contact pressures take a form similar in shape to the limit line of q_{ult} (Figures 7.18 and 7.19).

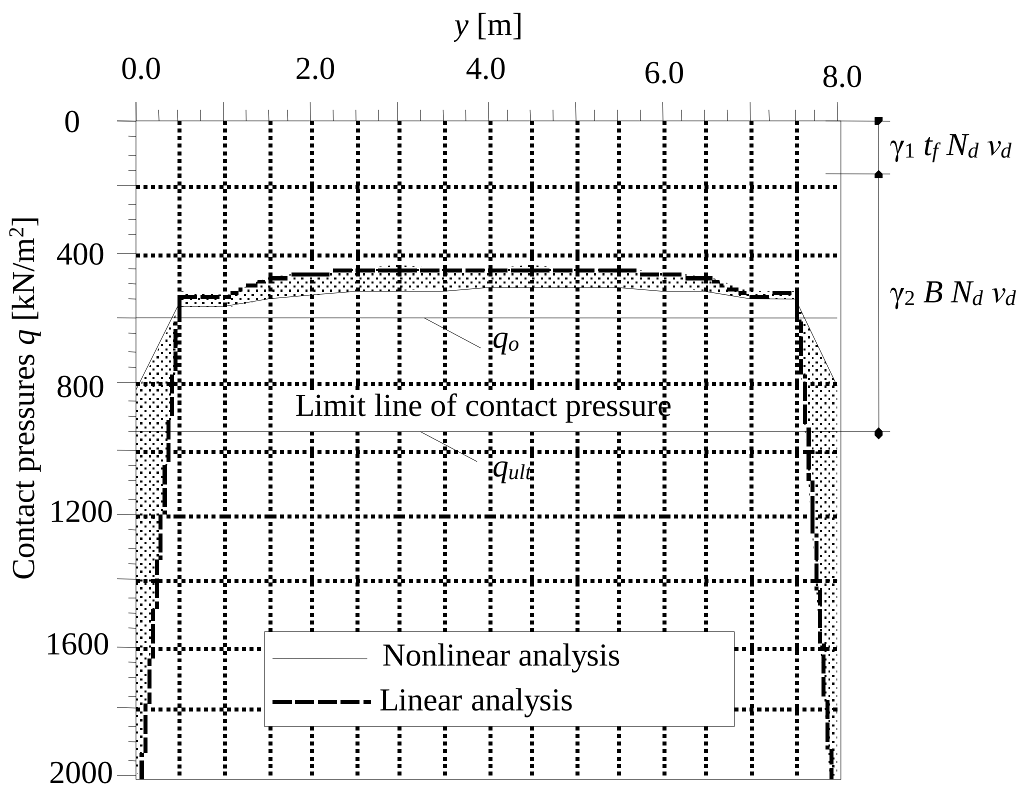

Figure 7.16 Contact pressures q [kN/m^2] at section a-a with and without limitation (Elastic raft - uniform ultimate bearing capacity)

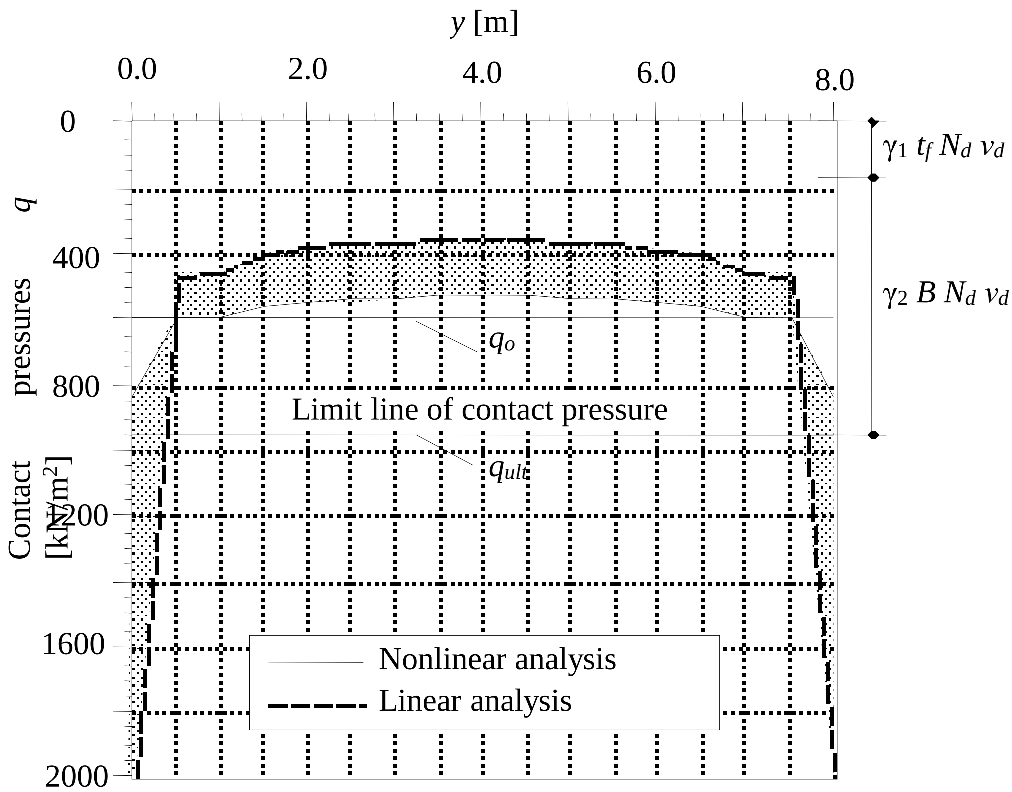

Figure 7.17 Contact pressures q [kN/m^2] at section a-a with and without limitation (Rigid raft - uniform ultimate bearing capacity)

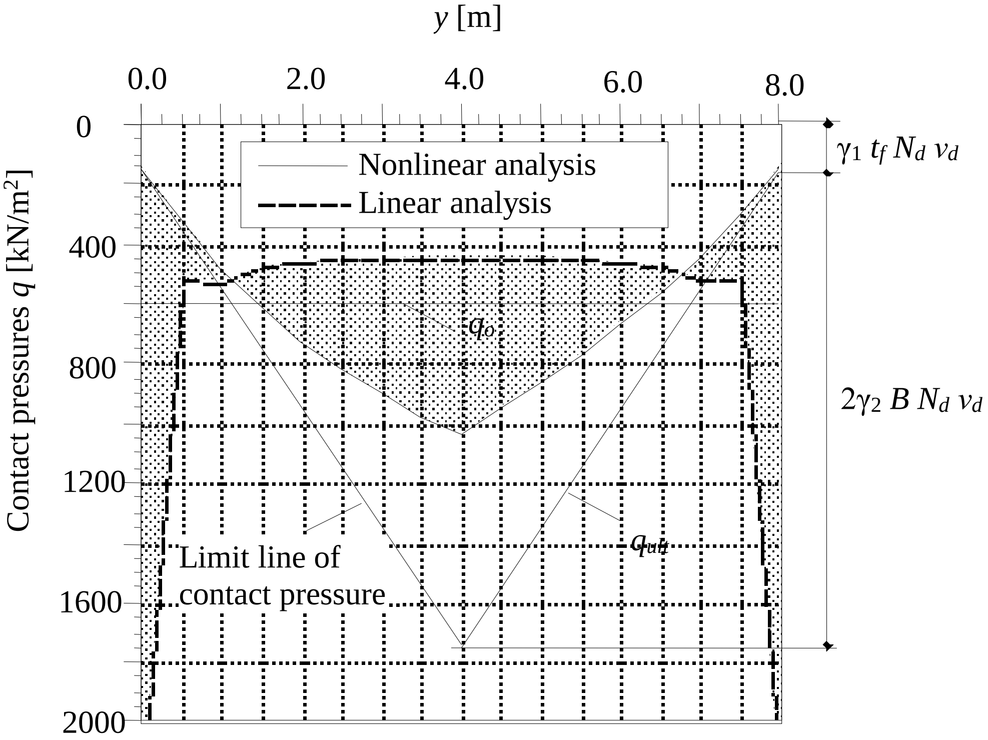

<u>Figure 7.18</u> Contact pressures q [kN/m^2] at section a-a with and without limitation (Elastic raft - variable ultimate bearing capacity)

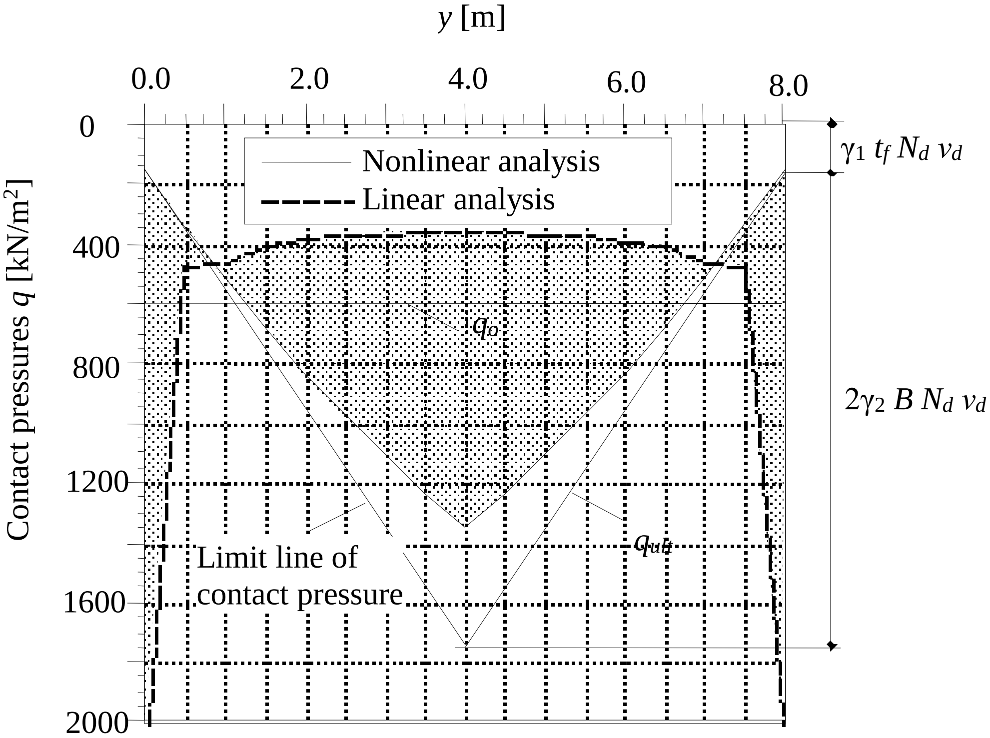

<u>Figure 7.19</u> Contact pressures q [kN/m^2] at section a-a with and without limitation (Rigid raft - variable ultimate bearing capacity)

The effect of redistribution of contact pressures on the moments m_y at section a-a of the raft is indicated in Figure 7.20 for case of uniform q_{ult} and in Figure 7.21 for case of variable q_{ult}. The Figures show that due to the redistribution of the contact pressures under the raft, the moments are considerably changed. In case of variable q_{ult}, not only the moments are changed but also the sign of moments. In case of uniform q_{ult}, the maximum moment m_y is reduced to 81 [%], while that in case of variable q_{ult} is reduced to more than double.

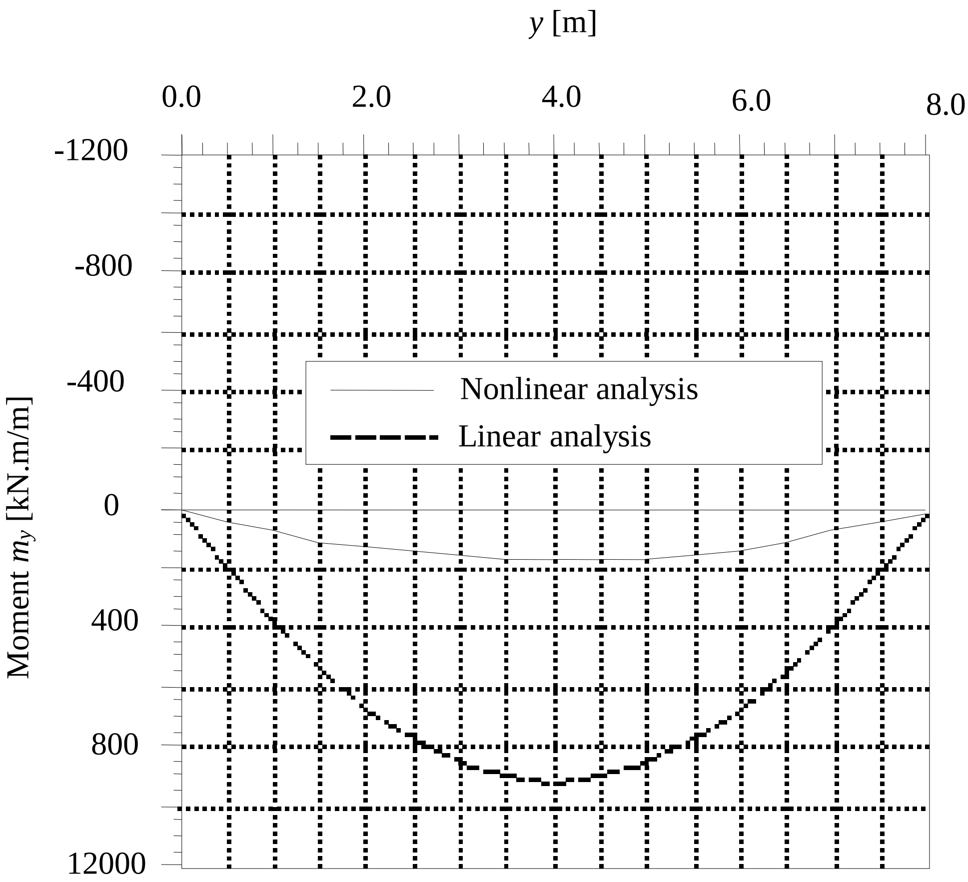

Figure 7.20 Moment m_y [kN.m/m] at section a-a with and without limitation (Elastic raft - uniform ultimate bearing capacity)

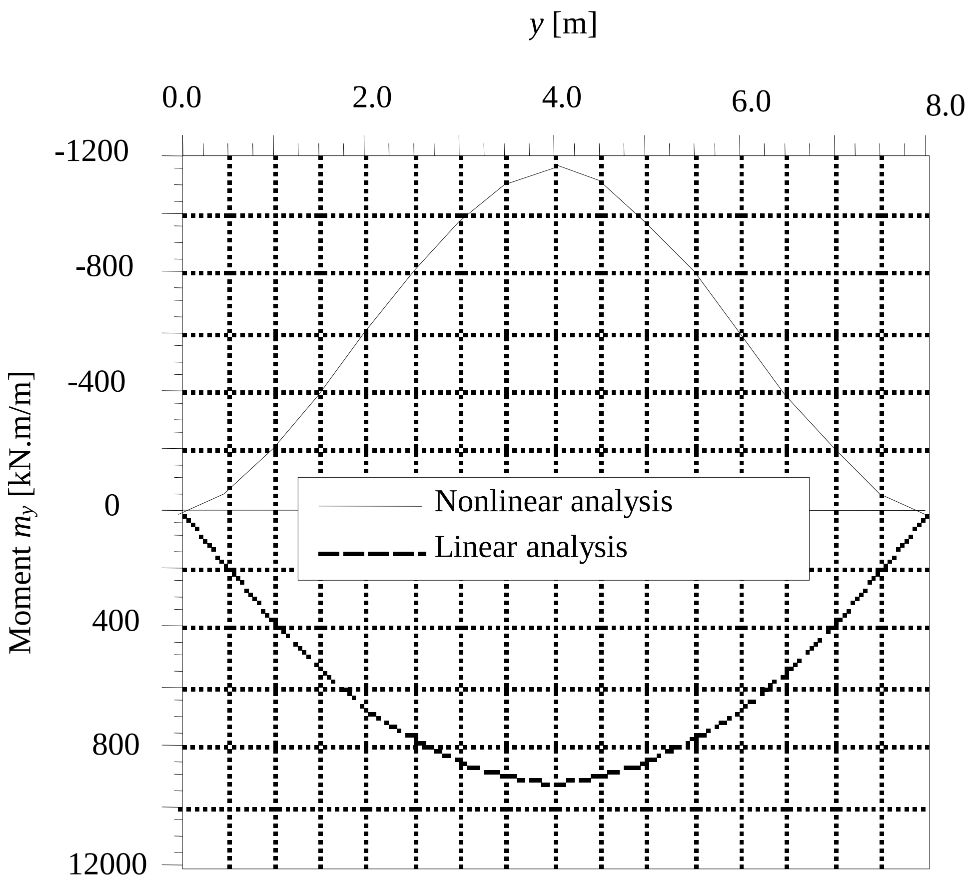

<u>Figure 7.21</u> Moment m_y [kN.m/m] at section a-a with and without limitation (Elastic raft - variable ultimate bearing capacity)